NJC

CF_x Primary Batteries Based on Fluorinated Carbon Nanocages

Journal:	*New Journal of Chemistry*
Manuscript ID	NJ-LET-06-2019-002956.R1
Article Type:	Letter
Date Submitted by the Author:	03-Jul-2019
Complete List of Authors:	Sosunov, Aleksei; Perm State University, department of solid state phys Ziolkowska, Dominika; Conn Center for Renewable Energy Research; University of Warsaw, Chemistry Department Ponomarev, Roman; Perm State University Henner, Viktor; Universiyty of Louisville Karki, Bhupendra; Universiyty of Louisville, Physics Smith, Nathan; Universiyty of Louisville Sumanasekera, Gamini; University of Louisville, Physics Jasinski, Jacek; Universiyty of Louisville, Conn Center for Renewable Energy Research

LETTER

CF_x Primary Batteries Based on Fluorinated Carbon Nanocages

Aleksei V. Sosunov,[a] Dominika A. Ziolkowska,[b,c] Roman S. Ponomarev,[a] Viktor K. Henner,[a,d] Bhupendra Karki,[d] Nathan Smith,[d] Gamini Sumanasekera[b,d] and Jacek B. Jasinski *[b]

Received 00th January 20xx,
Accepted 00th January 20xx

DOI: 10.1039/x0xx00000x

Fluorinated carbon nanocages were prepared using plasma treatment and were tested electrochemically in primary Li/CF_x batteries. A systematic increase of F/C ratio and specific capacity was obtained with increase of fluorination time. For the highest fluorinated material (x = 0.98), the specific capacity reached 850 $mAhg^{-1}$, i.e., theoretical value predicted for this composition.

Carbon materials, especially many of their nanostructured forms, are widely used in various technologies due to their unique properties, high performance, and low cost[1]. Porous nanocarbons in particular, which offer high stability, good electrical conductivity, large surface area and flexibility in terms of their pore structure design, are used as electrode materials in many electrochemical energy storage applications[2]. The properties of carbons can be tailored further by functionalization. This can be done using either weak π-π or van der Waals interactions or through a covalent bonding, which involves changes of carbon hybridized sp^2 orbitals. One the easiest functionalization methods is hydrogenation, where the attachment of hydrogen to a graphitic surface causes re-hybridization of the carbon atoms from a sp^2 to a distorted sp^3 configuration[3]. However, hydrogen binds to carbon relatively weakly, which leads to high-temperature stability issues. Therefore, there has been a significant interest in using fluorination as one of the most effective ways to modify physical and chemical properties of carbon materials[4, 5]. Because of its highest electronegativity, fluorine can form strong bonds with carbon. During direct fluorination, when carbon materials are treated with gaseous fluorine, both ionic and covalent bonds can be formed[6-9]. The ionic bonds are formed during intercalation of graphitic layers with fluorine. Additionally, especially at high concentrations, fluorine can also form covalent bonds with carbon and significantly alter physicochemical properties of the material. In recent years, numerous studies have been conducted on the fabrication and applications of fluorinated carbons[10-16]. Fluorinated nanostructured carbons have been used as promising electrode materials for electrochemical energy storage technologies[10]. Lithium/carbon fluoride (CF_x) primary batteries, as compared to other lithium battery chemistries, typically delivers higher gravimetric energy density, higher volumetric energy density, a wider temperature range, exceptional shelf-life, remarkably good safety record, extremely low self-discharge, and optimum price/performance[1,9]. The overall discharge reaction in these batteries can be expressed as $CF_x + xLi \rightarrow C + xLiF$ [17]. They are found in a wide range of applications for military[2], aerospace[3], electronics[4]. They are also very attractive for medical applications due to their relatively flat discharge profile, low internal resistance, and light weight[5, 6,8]. One of the main challenges for this technology is to increase the energy capacity of these batteries with the choice of a novel and low-cost material as the cathode. Traditional CF_x based cathode materials are formed by high-temperature intercalation of fluorine gas into graphite powder[7] paving the way for high energy density (250 Wh/kg), 7-year shelf-life primary batteries. Here, we report the fabrication and electrochemical testing of a new cathode material for Li/CF_x technology based on fluorination of ultrafine (~2.5 nm) bilayer carbon nanocages (CNCs), a novel carbon nanostructured material, synthesized using a simple, scalable, and cost-effective method, that has been developed in our group, recently[18]. Samples of such CNCs, synthesized following the procedure described by Ziolkowska et al[18], were fluorinated between 5- and 30-hours using fluorine radiofrequency plasma in a custom-designed, split-ring capacitively-coupled radio frequency (RF) plasma system with 13.56 MHz frequency and 200 W of maximum plasma power (Fig. 1). The fluorine source was tetrafluoromethane (CF_4), which is an odourless, colourless, and non-flammable liquefied gas. Although it should be handled carefully inside a fume hood with proper ventilation and a leak-free gas handling system, CF_4

[a] Perm State University, Perm, 614990 Russia.
[b] Conn Center for Renewable Energy Research, University of Louisville, Louisville, KY, 40292, USA. E-mail: jacek.jasinski@louisville.edu; Tel: +1-502 852 6338.
[c] Faculty of Chemistry, University of Warsaw, Pasteura 1, 02-093 Warsaw, Poland.
[d] Department of Physics and Astronomy, University of Louisville, Louisville, KY, 40292, USA.

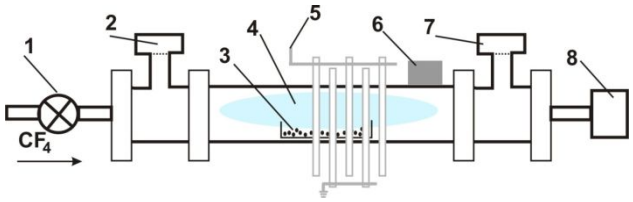

Fig. 1 Schematic setup of fluorination process. 1 - gas, 2 - gas flow controller, 3 - sample, 4 - plasma, 5 - radio frequency power source, 6 - vibrator, 7 - pressure sensor, 8 – pump.

is non-toxic compared to an elemental fluorine gas used typically to produce CF_x materials. For the fluorination, the CNCs were loaded into a ceramic crucible and placed at the centre of the plasma rings. The system was first slowly pumped down to a pressure of 200 mTorr. CF_4 gas was then introduced and the plasma was turned on. The flow rate of CF_4 gas was adjusted between 4-5 sccm and the plasma power was maintained between 100 W to 150 W to sustain the strongest plasma possible for the experiment without overheating of the system. While the sample was undergoing the fluorination, a vibrating motor was used to shake the sample and redistribute the material to ensure that the entire sample was fluorinated uniformly. Once the desired fluorination duration was achieved, the plasma system was turned off, vented and the fluorinated CNCs were removed and ready to use for the subsequent cathode fabrication.

The morphology, structure, and chemical composition of the pristine and fluorinated CNC samples was analysed using (scanning) transmission electron microscopy ((S)TEM), Raman spectroscopy, x-ray diffraction (XRD), and x-ray photoemission spectroscopy (XPS). A field emission gun (FEG) 200kV FEI Tecnai F20 transmission electron microscope was used for the (S)TEM study and a Bruker D8 Discovery for XRD measurements. A VG Scientific MultiLab 3000 ultra-high vacuum surface analysis system, with the base pressure in the 10^{-8} Torr range and and Al K_α (1486.6 eV) x-ray source was used for the XPS data collection. Raman spectra were collected using a Renishaw inVia Raman microscope system and a 632 nm He-Ne laser.

CF_x electrodes were prepared by combining fluorinated CNCs with a binder (carbon black coated with Teflon with the ratio of 3:1). The carbon binder was added to ensure good electrical conductivity. The active material and carbon binder were thoroughly mixed in a mortar with a few drops of ethanol to a homogenous paste, shaped in the form of a thin disc and subsequently pressed into stainless steel mesh, yielding a CF_x cathode. The CF_x batteries were prepared in a two-electrode system using a coin cell assembly. A 1M solution of lithium hexafluorophosphate ($LiPF_6$) salt dissolved in propylene carbonate (PC) was used as the electrolyte. The cells were assembled in the glove box environment (argon filled). The cell parts were dried in the vacuum furnace at 200 ^oC for 2 hours and inserted to the glovebox in the sealed tube. A piece of lithium foil was pressed into the stainless-steel mesh, making the lithium anode. The separator (Celgard) soaked with the electrolyte was next placed on top of the anode. Next, the CF_x cathode was placed on top of the separator. After the battery components were assembled, the battery was crimped to ensure proper sealing. Electrochemical measurements were performed using a Pine Research Instrumentation WaveDriver20 Bipotentiostat/ Galvanostat System.

Fig. 2 shows the high-angle annular dark-field (HAADF)-STEM image and elemental maps of carbon, oxygen, and fluorine of 1hr fluorinated CNC sample. It is clear from the elemental maps that fluorine is homogeneously incorporated into the CNC structure and follows the distribution of carbon and oxygen. Both, oxygen and fluorine are incorporated in the form of functional groups in the CNC structure. The functional oxygen groups are formed during the synthesis of CNCs, as discussed in the XPS analysis.

Fig. 3a shows the XPS survey scans for progressively fluorinated CNC samples. The characteristic peaks of fluorine, carbon, and oxygen, namely F1s, C1s and O1s, are indicated. The signature of fluorine, the F1s peak, is not present for the pristine CNCs sample, but starts to appear for 5 hours fluorinated sample and its intensity grows gradually with the fluorination time, as observed for the 15- and 30-hours fluorinated samples. With the gradual increase in the area of the fluorine peak, the carbon peak simultaneously diminished. The peak deconvolution of the high-resolution C1s for all four analysed samples is shown in Fig. 3b. The evolution of carbon bonding and the changing of functionalization is clearly observed with the increasing level of fluorination[18-21]. For the 5-hour sample a weak C-F component peak starts to be observed. Its intensity increases significantly for the 15 hour sample and even more so for the 30 hours sample. Additionally, $-CF_2$ and $-CF_3$ peaks are well-developed for the 30 hours sample[22-24]. Fig. 3c shows the elemental concertation data obtained from the quantification of the survey spectra shown in Fig. 3a. The value x of these CFx materials evaluated from the fluorine to carbon concertation ratio was estimated at 0, 0.04, 0.22, and 0.98, for 0, 5, 15, and 30 hours of fluorination, respectively. XRD patterns of fluorinated samples are shown in Fig. S1. The XRD pattern of the pristine sample display the presence of two peaks at 44.6^o and 77.3^o assigned to (100) and (110) reflections and in good agreement with the previous literature[18]. It is clear that fluorination reduces intensity of both the peaks due to the gradual degradation of the graphite-like structure of the

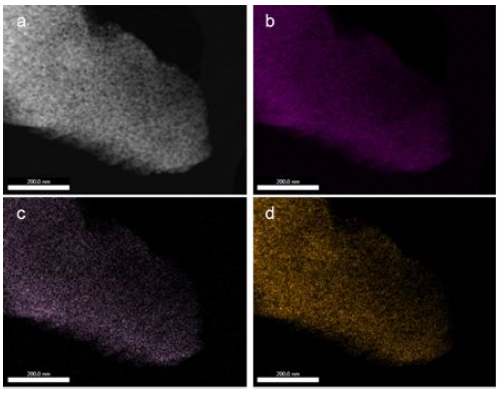

Fig. 2 Elemental mapping of CNC-F. HAADF-STEM image (a) and elemental maps of carbon (b), oxygen (c), and fluorine (d).

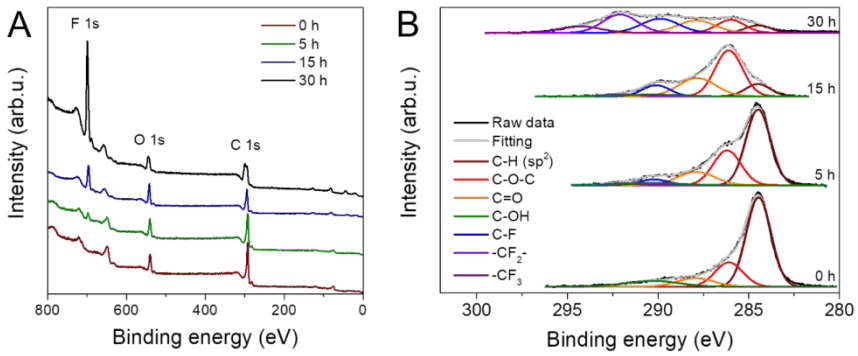

C

%Atom	Pristine	5h	15h	30h
C	83.6	79.7	62.2	45.4
O	16.4	17.1	24.1	10
F	-	3.2	13.6	44.6

Fig. 3 XPS analysis of fluorinated CNCs: (a) XPS survey spectra, (b) peak deconvolution of high-resolution XPS C1s spectra, and (c) carbon, oxygen, and fluorine concentration obtained from the survey spectra quantification.

pristine CNCs. This is also consistent with the high-resolution TEM analysis of these samples (Fig. 2S).

Fig. 4a shows the Raman spectra of pristine and progressively fluorinated CNCs samples. The characteristic D and G bands along with weaker 2D and D+G bands are seen in all 4 samples[18, 25-27]. Spectral deconvolution using Lorentzian line shape performed after background removal is also shown in each spectrum. These four lines are located at 1326, 1590, 2650 and 2900 cm-1, respectively. The D/G, 2D/G, and 2D/D peak intensity ratios obtained for these 4 samples are plotted in Fig. 4b. Interestingly, only small variations are observed with the increasing fluorination time. Based on XPS findings it was expected that the fluorinated carbon should possesses even more of the disorder structure, especially for the samples fluorinated for 30 hrs. This trend is visible by an increase in the D/G lines ratio from ~2.3 for pure CNCs to ~2.4 for a 30 h fluorinated CF_x. This change is much smaller than the surface modifications shown in XPS spectra. This suggests that the fluorination process affect mostly the top graphitic layers of the carbon particles. Fig. 5 shows the specific capacity for each sample with varying levels of fluorination (pristine, 5 hours, 15 hours, and 30 hours). The primary battery with the highest amount of fluorination was able to reach a specific capacity of 850 $mAhg^{-1}$ whereas the battery without any fluorine had a specific capacity of only 72 $mAhg^{-1}$. The 5 hours of fluorination yielded the specific capacity of 123 $mAhg^{-1}$ and the 15 hours of fluorination led to a capacity as high as 304 $mAhg^{-1}$. A longer fluorination time positively induces an additional specific capacity of the final material.

The specific capacity of the Li/CF_x battery depends on the x, i.e., the F/C ratio. For material with x = 1, theoretical capacity is 865 $mAhg^{-1}$ [28, 29]. The specific capacity of our 30-hour sample, matches almost exactly the theoretical capacity calculated for the F/C ratio of x = 0.98, i.e., the ratio measured for this sample. Based on the tap density of 0.602 g/cm^{-3} (Supporting Information), the obtained capacity value of 850 $mAhg^{-1}$ corresponds to 1700 Wh/kg and 2824 Wh/L at 2 V. This is one of the highest ever reported for a nanostructured CF_x material. Only in the case of specially-designed systems with additional synergistic effects, such a Li/CF_x battery based on graphene co-

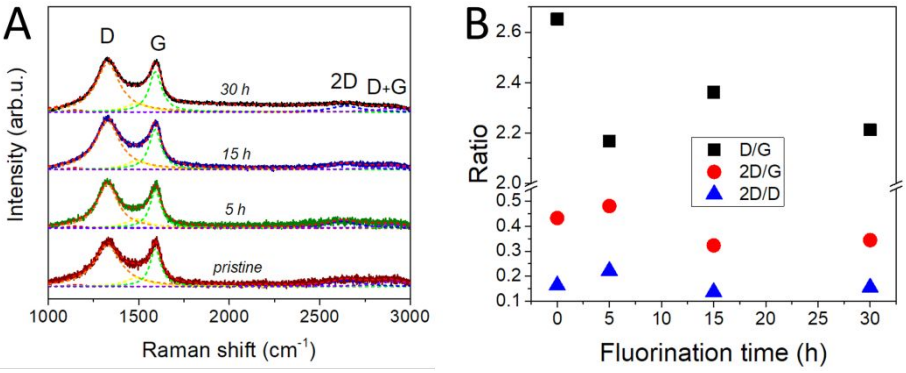

Fig. 4 Raman spectra (a) and Raman peak intensity ratios (b) of pristine and progressively fluorinated CNCs samples.

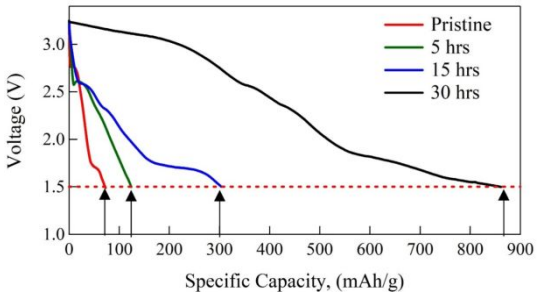

Fig. 5 First cycle discharge capacity curves of CF_x primary lithium battery for varying fluorine concentrations (current density 100 mA g^{-1}).

doped with fluorine and nitrogen[30] or a solid-state Li/CF_x battery with a solid electrolyte of Li_3PS_4[29], the higher specific capacities, beyond the theoretical limit, namely 1075 and 1095 $mAhg^{-1}$, respectively, have been reported. By extension, the combination of either of these two strategies, i.e., co-doping or application of solid-state electrolyte, with our nanostructured carbon in the form of CNCs, may lead to even higher capacity values of Li/CF_x batteries.

Fluorinated CNCs were tested against Li as the cathode material in CF_x primary batteries. These materials showed systematically increased F/C ratio, i.e., x value in the CF_x formula, and specific capacity value with increase of the fluorination time. The CNCs fluorinated for 30 hours reached its highest fluorination level of x = 0.98 and showed capacity of 850 $mAhg^{-1}$, i.e., the theoretical capacity calculated for this x value. The findings suggest that primary Li/CF_x batteries with capacities exciding the theoretical limit can be obtained by co-doping of fluorinated CNCs and/or by application of solid-state electrolyte system.

Conflicts of interest

The authors declare no conflict of interest.

Acknowledgements

Energy Research and funding from the US National Science Foundation EPSCoR Program (sub-award no. 3048111570-15-016). This research was also supported by the RFBR grant 17-42-590271 and Perm Krai Ministry of Science and Education grant C-26/798.

Notes and references

1. L. Dai, D. W. Chang, J. B. Baek and W. Lu, *Small*, 2012, **8**, 1130-1166.
2. Z. Yang, J. Ren, Z. Zhang, X. Chen, G. Guan, L. Qiu, Y. Zhang and H. Peng, *Chemical Reviews*, 2015, **115**, 5159-5223.
3. D. C. Elias, R. R. Nair, T. Mohiuddin, S. Morozov, P. Blake, M. Halsall, A. Ferrari, D. Boukhvalov, M. Katsnelson and A. Geim, *Science*, 2009, **323**, 610-613.
4. S. D. Sherpa, J. Kunc, Y. Hu, G. Levitin, W. A. De Heer, C. Berger and D. W. Hess, *Applied Physics Letters*, 2014, **104**, 081607.
5. B. Wang, J. Wang and J. Zhu, *ACS Nano*, 2014, **8**, 1862-1870.
6. A. P. Kharitonov and L. N. Kharitonova, *Pure Appl. Chem.*, 2009, **81**, 451-471.
7. A. P. Kharitonov, *Prog. Org. Coat.*, 2008, **61**, 192-204.
8. P. A. B. Carstens, S. A. Marais and C. J. Thompson, *Journal of Fluorine Chemistry*, 2000, **104**, 97-107.
9. S. Zhou, S. D. Sherpa, D. W. Hess and A. Bongiorno, *J. Phys. Chem. C*, 2014, **118**, 26402-26408.
10. T. Nakajima, S. Shibata, K. Naga, Y. Ohzawa, A. Tressaud, E. Durand, H. Groult and F. Warmont, *J. Power Sources*, 2007, **168**, 265-271.
11. T. Nakajima, *Journal of Fluorine Chemistry*, 2007, **128**, 277-284.
12. T. Nakajima, *Solid State Sci.*, 2007, **9**, 777-784.
13. A. Panahi and M. H. Sabour, *Chem. Eng. Sci.*, 2017, **173**, 60-73.
14. W. Feng, P. Long, Y. Y. Feng and Y. Li, *Adv. Sci.*, 2016, **3**, 22.
15. J. Y. Jung, H. R. Yu, S. J. In, Y. C. Choi and Y. S. Lee, *J. Nanomater.*, 2013, 6.
16. D. Claves, *New J. Chem.*, 2011, **35**, 2477-2482.
17. S. S. Zhang, D. Foster, J. Wolfenstine and J. Read, *J. Power Sources*, 2009, **187**, 233-237.
18. D. Ziolkowska, J. Jangam, G. Rudakov, T. Paronyan, M. Akhtar, G. Sumanasekera and J. Jasinski, *Carbon*, 2017, **115**, 617-624.
19. M. Jana, P. Khanra, N. C. Murmu, P. Samanta, J. H. Lee and T. Kuila, *Physical Chemistry Chemical Physics*, 2014, **16**, 7618-7626.
20. F. Xiao, S. Yang, Z. Zhang, H. Liu, J. Xiao, L. Wan, J. Luo, S. Wang and Y. Liu, *Scientific Reports*, 2015, **5**, 9359.
21. S. P. Lim, A. Pandikumar, Y. S. Lim, N. M. Huang and H. N. Lim, *Scientific Reports*, 2014, **4**, 5305.
22. S.-M. Yun, J.-W. Kim, M.-J. Jung, Y.-C. Nho, P.-H. Kang and Y.-S. Lee, *Carbon Letters*, 2007, **8**, 292-298.
23. A. Cordeiro, M. Nitschke, A. Janke, R. Helbig, F. D'Souza, G. Donnelly, P. Willemsen and C. Werner, *Express Polymer Letters*, 2009, **3**, 70-83.
24. M. S. Loeian, D. A. Ziolkowska, F. Khosravi, J. B. Jasinski and B. Panchapakesan, *Scientific Reports*, 2017, **7**, 14599.
25. M. Dresselhaus, A. Jorio and R. Saito, *Annu. Rev. Condens. Matter Phys.*, 2010, **1**, 89-108.
26. A. C. Ferrari, *Solid State Comm.*, 2007, **143**, 47-57.
27. A. C. Ferrari and J. Robertson, *Philosophical Transactions of the Royal Society of London. Series A: Mathematical, Physical and Engineering Sciences*, 2004, **362**, 2477-2512.
28. Q. Zhang, S. d'Astorg, P. Xiao, X. Zhang and L. Lu, *J. Power Sources*, 2010, **195**, 2914-2917.
29. E. Rangasamy, J. Li, G. Sahu, N. Dudney and C. Liang, *Journal of the American Chemical Society*, 2014, **136**, 6874-6877.
30. S. Huang, Y. Li, Y. Feng, H. An, P. Long, C. Qin and W. Feng, *Journal of Materials Chemistry A*, 2015, **3**, 23095-23105.

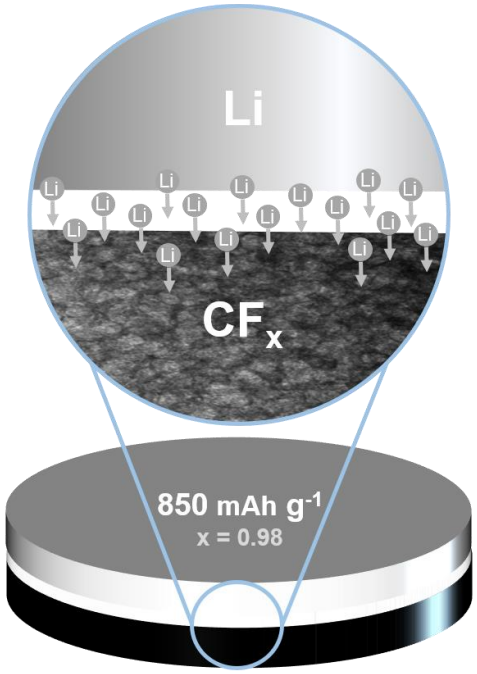

The material with the fluorination level of x = 0.98 reaches the specific capacity of 850 $mAhg^{-1}$, i.e., its theoretical value.